2002

Participation of Two Members of the Very Long-chain Acyl-CoA Synthetase Family in Bile Acid Synthesis and Recycling

Stephanie J. Mihalik

Steven J. Steinberg

Zhengtong Pei

Joseph Park

Do G. Kim

See next page for additional authors

Recommended Citation

Mihalik, Stephanie J., Steven J. Steinberg, Zhengtong Pei, Joseph Park, Do G. Kim, Ann K. Heinzer, Georges Dacremont et al. "Participation of two members of the very long-chain acyl-CoA synthetase family in bile acid synthesis and recycling." Journal of Biological Chemistry 277, no. 27 (2002): 24771-24779.

THE JOURNAL OF BIOLOGICAL CHEMISTRY
Vol. 277, No. 27, Issue of July 5, pp. 24771–24779, 2002

Printed in U.S.A.

Participation of Two Members of the Very Long-chain Acyl-CoA Synthetase Family in Bile Acid Synthesis and Recycling*

Received for publication, April 5, 2002
Published, JBC Papers in Press, April 29, 2002, DOI 10.1074/jbc.M203295200

Stephanie J. Mihalik‡§, Steven J. Steinberg‡¶, Zhengtong Pei‡¶, Joseph Park‡, Do G. Kim‡, Ann K. Heinzer‡, Georges Dacremont‖, Ronald J. A. Wanders, Dean A. Cuebas‡‡, Kirby D. Smith‡§, and Paul A. Watkins‡¶§§**

*From the ‡Kennedy Krieger Institute and the Departments of §Pediatrics and ¶Neurology, Johns Hopkins University School of Medicine, Baltimore, Maryland 21205, the ‖Department of Pediatrics, Ghent University School of Medicine, B-9000 Ghent, Belgium, the **Laboratory of Genetic Metabolic Diseases, Academic Medical Center, 1105 AZ Amsterdam, The Netherlands, and the ‡‡Department of Chemistry, Southwest Missouri State University, Springfield, Missouri 65804*

Bile acids are synthesized *de novo* in the liver from cholesterol and conjugated to glycine or taurine via a complex series of reactions involving multiple organelles. Bile acids secreted into the small intestine are efficiently reabsorbed and reutilized. Activation by thioesterification to CoA is required at two points in bile acid metabolism. First, 3α,7α,12α-trihydroxy-5β-cholestanoic acid, the 27-carbon precursor of cholic acid, must be activated to its CoA derivative before side chain cleavage via peroxisomal β-oxidation. Second, reutilization of cholate and other C_{24} bile acids requires reactivation prior to re-conjugation. We reported previously that homolog 2 of very long-chain acyl-CoA synthetase (VLCS) can activate cholate (Steinberg, S. J., Mihalik, S. J., Kim, D. G., Cuebas, D. A., and Watkins, P. A. (2000) *J. Biol. Chem.* 275, 15605–15608). We now show that this enzyme also activates chenodeoxycholate, the secondary bile acids deoxycholate and lithocholate, and 3α,7α,12α-trihydroxy-5β-cholestanoic acid. In contrast, VLCS activated 3α,7α,12α-trihydroxy-5β-cholestanoate, but did not utilize any of the C_{24} bile acids as substrates. We hypothesize that the primary function of homolog 2 is in the reactivation and recycling of C_{24} bile acids, whereas VLCS participates in the *de novo* synthesis pathway. Results of *in situ* hybridization, topographic orientation, and inhibition studies are consistent with the proposed roles of these enzymes in bile acid metabolism.

The synthesis of bile acids from cholesterol is a complex process requiring modifications of both the steroid nucleus and the aliphatic side chain (reviewed in Refs. 1 and 2). Cholic acid and chenodeoxycholic acid, the two primary bile acids in humans, are synthesized in the liver via the concerted action of enzymes located in the endoplasmic reticulum, cytosol, mitochondria, and peroxisomes. The immediate precursors of the C_{24} bile acids cholate and chenodeoxycholate are the C_{27} compounds 3α,7α,12α-trihydroxy-5β-cholestanoic acid (THCA)[1] and 3α,7α-dihydroxy-5β-cholestanoic acid (DHCA), respectively (1, 2). It is well established that chain shortening of the methyl-branched side chain of THCA and DHCA by β-oxidation takes place in peroxisomes (3). For β-oxidation to occur, THCA and DHCA must first be activated to their CoA thioesters. The products of chain shortening are choloyl-CoA and chenodeoxycholoyl-CoA and not the free bile acids (4).

The CoA thioesters of the primary bile acids are conjugated to the amino acid glycine or taurine in the hepatocyte before secretion into the bile canaliculi (1, 2). After bile secretion into the intestine during digestion, the conjugated primary bile acids are subject to deconjugation, 7α-dehydroxylation, and other modifications by the intestinal flora (1, 5). 7α-Dehydroxylation converts conjugated or unconjugated cholate to deoxycholate, and chenodeoxycholate to lithocholate. Deoxycholate and lithocholate are referred to as secondary bile acids. A substantial portion of the intestinal bile acid pool is reabsorbed by passive diffusion throughout the small bowel and by active transport in the distal ileum; all of these compounds return to the liver via the enterohepatic circulation for reutilization (6). Recycled unconjugated primary and secondary bile acids must then be re-conjugated to glycine or taurine before return to the bile. However, re-conjugation can occur only after the free acids are activated to their CoA derivatives.

We recently demonstrated that human very long-chain acyl-CoA synthetase homolog 2 (hVLCS-H2), a liver-specific member of the protein family that includes very long-chain acyl-CoA synthetases (VLCSs) and fatty acid transport proteins, is a choloyl-CoA synthetase (7). We hypothesized that a major function of this protein is to activate recycled bile acids prior to their re-conjugation. In this report, we provide further evidence for a role for hVLCS-H2 in activation of primary and secondary bile acids. Furthermore, we demonstrate that hVLCS and hVLCS-H2 are capable of activating the cholic acid precursor (THCA) and speculate on the complementary role of these proteins in bile acid synthesis. Based on the substrate specificity of hVLCS-H2, we will hereafter refer to this protein as human bile acyl-CoA synthetase (hBACS).

* This work was supported by National Institutes of Health Grants NS10533, NS37355, HD10981, and HD24061. The costs of publication of this article were defrayed in part by the payment of page charges. This article must therefore be hereby marked "*advertisement*" in accordance with 18 U.S.C. Section 1734 solely to indicate this fact.

The nucleotide sequence(s) reported in this paper has been submitted to the GenBank™/EBI Data Bank with accession number(s) AF033031.

§§ To whom correspondence should be addressed: Kennedy Krieger Inst., Johns Hopkins University School of Medicine, 707 N. Broadway, Baltimore, MD 21205. Tel.: 410-502-9030; Fax: 410-502-8279; E-mail: watkins@kennedykrieger.org.

[1] The abbreviations used are: THCA, 3α,7α,12α-trihydroxy-5β-cholestanoic acid; DHCA, 3α,7α-dihydroxy-5β-cholestanoic acid; hVLCS, human very long-chain acyl-CoA synthetase; hVLCS-H1 and hVLCS-H2, hVLCS homologs 1 and 2, respectively; hBACS, human bile acyl-CoA synthetase; EST, expressed sequence tag; HPLC, high-performance liquid chromatography; rACS1, rat liver long-chain acyl-CoA synthetase-1.

EXPERIMENTAL PROCEDURES

Materials and General Methods—Sodium salts of cholic, chenodeoxycholic, deoxycholic, and lithocholic acids were obtained from either Steraloids, Inc. (Wilton, NH) or Sigma. [1-^{14}C]Cholic acid (55 mCi/mmol) and [1-^{14}C]chenodeoxycholic acid (51.3 mCi/mmol) were obtained from American Radiolabeled Chemicals. [1-^{14}C]Palmitic acid (50 mCi/mmol) was from Moravek Biochemicals, Inc. The PCR conditions were as previously described (8). Protein was determined by the method of Lowry *et al.* (9).

Synthesis of THCA and [26-^{14}C]THCA—Δ24-THCA was synthesized by the method of Xu and Cuebas (10). Unlabeled THCA was prepared by the catalytic hydrogenation of Δ24-THCA using Adams' catalyst (Aldrich) suspended in methanol at 1-atmosphere pressure for 12 h. The product is a racemic mixture of (25*S*)- and (25*R*)-THCA stereoisomers. [26-^{14}C]THCA was prepared from THCA by a modification of the method of Tserng and Klein (11). THCA was formylated to protect the hydroxyl groups by heating 0.24 mmol in 1 ml of 90% formic acid containing 0.025 ml of 70% perchloric acid for 2 h at 55 °C. After cooling to ~45 °C and dropwise addition of acetic anhydride until massive bubbling occurred, the solution was further cooled to room temperature, and the formylated THCA was extracted with diethyl ether and dried (85% yield). The corresponding 25-chloronorcholane was then obtained by dissolving 0.2 mmol of the formylated THCA in 2.5 ml of dry benzene containing 0.4 mmol of lead tetraacetate and 0.4 mmol of LiCl and heating to 85 °C for 3 h. At this time and again at 4 h, 0.2 mmol of LiCl was added. The reaction mixture was then cooled, centrifuged to remove precipitated material, washed with ice-cold 2% NaOH and ice-cold water, dried with $MgSO_4$, and evaporated to dryness to afford 25-chloro-3α,7α,12α-triformyloxynorcholane (75% yield). 40 μmol of this product was dissolved in 1 ml of dry dimethyl sulfoxide containing 2.0 mCi of Na^{14}CN (36 μmol, 55 mCi/mmol) and heated for 32 h at 70 °C. After cooling, 1 ml of 2 N NaOH was added, and the solution was heated to 90 °C for 1 h to hydrolyze the formyl groups. The product (cyano-3α,7α,12α-trihydroxy[26-^{14}C]norcholane) was then extracted with chloroform, dried, and purified by preparative thin-layer chromatography in cyclohexane/ethyl acetate/acetic acid (21:69:9; 1.55 mCi; 77% yield). Finally, the purified nitrile was dissolved in 2 ml of ethanol and 10% aqueous NaOH (2:1) and heated to 80 °C for 40 h. After cooling, the reaction mixture was concentrated to one-third of its original volume to remove ethanol and restored again to its original volume by adding water. After acidification, the reaction product was extracted with chloroform. Analysis by thin-layer and gas-liquid chromatography showed that the reaction product was identical to THCA (1.22 mCi; 79% yield).

Cloning and Expression of VLCS and BACS Constructs—Full-length cDNAs encoding hVLCS and hBACS were cloned into the expression vector pcDNA3 (Invitrogen) as previously described (8, 12). Cloning of N-*myc*-hBACS was also described previously (12).

For production of N-*myc*-hVLCS, the full-length open reading frame of hVLCS was amplified by PCR using oligonucleotide primers P0-17 (5′-CCCGTCGACCATGCTTTCCGCCATCTACA-3′, which incorporates a *Sal*I restriction site) and P0-4 (5′-GTCTGCGGCCGCCCTCCAA-CAAGCTCAGTTTGC-3′, which incorporates a *Not*I site) with hVLCS in pcDNA3 as template. The product was ligated into the *Xho*I and *Not*I sites of N-*myc*-pcDNA3, a modified pcDNA3 vector that places the c-*myc* epitope in-frame at the amino terminus (a gift of Dr. S. Gould).

To produce C-*myc*-hVLCS, a three-fragment ligation was performed. A 1614-bp fragment containing the initiator methionine codon was excised from hVLCS in pcDNA3 using *Bam*HI and *Bgl*I. A 550-bp fragment of hVLCS in which the stop codon was replaced by a *Hin*dIII restriction site was amplified by PCR using hVLCS in pcDNA3 as template and oligonucleotide primers P0-5 (5′-AGCAAAGGCTCA-GACAGAGA-3′, forward) and P0-19 (5′-CCGAAGCTTGAGTT-TCAGGGTTTTAGC-3′, reverse); this fragment was cut with *Bgl*I and *Hin*dIII, yielding a 477-bp fragment. These two pieces were ligated into the *Bam*HI and *Hin*dIII sites of pcDNA3.1-*myc*-HisA (Invitrogen), forming C-*myc*-hVLCS.

A similar approach was used to produce C-*myc*-hBACS. A 1801-bp fragment containing the start codon was excised from hBACS in pcDNA3 using *Kpn*I and *Nhe*I. A 422-bp fragment of hBACS in which the stop codon was replaced by a *Hin*dIII restriction site was amplified by PCR using hBACS in pcDNA3 as template with oligonucleotide primers P2-9 (5′-CGCCTCGGGGACACCTTC-3′, forward) and P2-18 (5′-TTTAAGCTTGAGCCTCCAGGTTCCCTC-3′, reverse); this fragment was cut with *Nhe*I and *Hin*dIII, yielding a 270-bp fragment. These two pieces were ligated into the *Kpn*I and *Hin*dIII sites of pcDNA3.1-*myc*-HisA, forming C-*myc*-hBACS.

Expressed sequence tag (EST) clones representing the murine homolog of hVLCS were identified by homology probing of the EST data base using rat VLCS cDNA sequence (13) as the query. An EST clone (GenBank™ accession number AA038113) containing the C-terminal 921 base pairs of the open reading frame plus 8 bp of the 3′-untranslated region was obtained from Genome Systems, Inc. The EST clone insert was moved to the mammalian cloning vector pcDNA3 using *Eco*RI and *Not*I. The 5′-untranslated region of rat VLCS (13) was used to design a forward PCR primer (5′-CGCGGGTACCGATCTCACCT-GACCCCAGACG-3′) with an engineered *Kpn*I site and to amplify the 5′-end of mouse VLCS from liver total cDNA with a reverse primer (5′-tgccttcagtggatgcgtagaac-3′). The ~1100-bp PCR product encompassed a second *Kpn*I site near the 3′-end. Both *Kpn*I sites in the PCR fragment were used to clone the PCR fragment into a *Kpn*I site near the 5′-end of EST AA038113 in pcDNA3, and the clone was re-sequenced. The full-length open reading frame of mouse VLCS was deposited in the GenBank™/EBI Data Bank (accession number AF033031).

The completed mouse VLCS cDNA sequence was used to search the EST data base for related mouse ESTs. ESTs AA106121 and AA538033 both contained full-length cDNA encoding the murine homolog of hBACS. The insert of EST AA106129 was released by digestion with *Acc*I and *Spe*I and was blunt-ended with Klenow enzyme. The fragment was then cloned into the *Eco*RV site of pcDNA3, and the clone was sequenced.

In most expression experiments, COS-1 cells (a gift of Dr. C. Thompson) were transfected with 10 μg of plasmid DNA by electroporation as described previously (8). In some experiments, cells were transfected using GeneSHUTTLE-40 (Qbiogene, Inc.). 10 μg of plasmid DNA was mixed with 30 μl of GeneSHUTTLE-40 and incubated with COS-1 cells in serum-free medium for 8 h. Following addition of an equal volume of culture medium containing 20% fetal bovine serum, cell incubation was continued for 16 h. At this time, the culture medium was replaced with culture medium containing 10% fetal bovine serum, and the cells were harvested 72 h post-transfection. Washed cell pellets were resuspended in 0.25 M sucrose containing 10 mM Tris (pH 8.0) and 1 mM EDTA, frozen at −80 °C for a minimum of 4 h, and thawed on ice for assay.

Indirect Immunofluorescence—COS-1 cells were transfected as described above with hVLCS or hBACS containing the c-*myc* epitope in-frame at either the N or C terminus of the protein. After 3 days, cells were fixed in 4% formaldehyde in phosphate-buffered saline and solubilized with either 1.0% Triton X-100 or 15 μg/ml digitonin prior to incubation with primary and secondary antibodies as described previously (14).

Bile Acyl-CoA Synthetase and Fatty Acyl-CoA Synthetase Assays—Both isotopic and high-performance liquid chromatography (HPLC)-based assays of bile acid activation were performed as previously described (7), with the following exceptions. The poorly soluble sodium salt of lithocholate was dried on the bottom of reaction tubes and was solubilized using 50 μl of β-cyclodextrin (10 mg/ml) in 10 mM Tris (pH 8.0) by brief sonication prior to addition of other reaction components and enzyme. In the experiments shown in Figs. 1*C* and 3*B*, the gradient program for elution of bile acyl-CoA derivatives from the reverse-phase HPLC column (25–65% solvent B over 30 min), which deviated from the previously described method (25–50% solvent B over 25 min) (7). The unlabeled THCA used in these experiments also contained Δ24-THCA (8%, w/w). In the HPLC tracing shown in Fig. 1*D*, peak 3 was tentatively identified as the CoA derivative of Δ24-THCA. The retention time of this product was identical to that of Δ24 THCA-CoA produced from the incubation of 24-hydroxy-THCA (varanoyl-CoA) with fibroblasts from patients with mutations in the 3-hydroxyacyl-CoA dehydrogenase domain of peroxisomal D-bifunctional protein. Tracings from patients with mutations in the enoyl hydratase portion of the gene had severe reductions in this product, as described previously (15). For inhibition experiments (see Fig. 3*B*), (25*S*)-THCA-CoA was quantitated using a Hewlett-Packard 3392A integrator. Activation of [1-^{14}C]palmitic acid by transfected COS-1 cells was measured as previously described (8).

In Situ Hybridization—The method of Giger *et al.* (16) was used, with modification. Plasmids containing full-length cDNA encoding the murine homologs of VLCS and BACS in pcDNA3 were linearized by cutting at a restriction site upstream of the initiator methionine codon (for antisense probes) or just downstream of the stop codon (for sense probes). Antisense RNA probes for VLCS (1865 bp) and BACS (2071 bp) were synthesized using digoxigenin-labeled UTP (Roche Molecular Biochemicals) and SP6 RNA polymerase (Ambion Inc.). The corresponding digoxigenin-labeled sense probes were synthesized for use as controls using T7 RNA polymerase (Ambion Inc.). Livers obtained from adult mice were quick-frozen in liquid nitrogen. Slices (8 μm) were obtained using a Microm HM500M cryostat, collected on Superfrost Plus slides

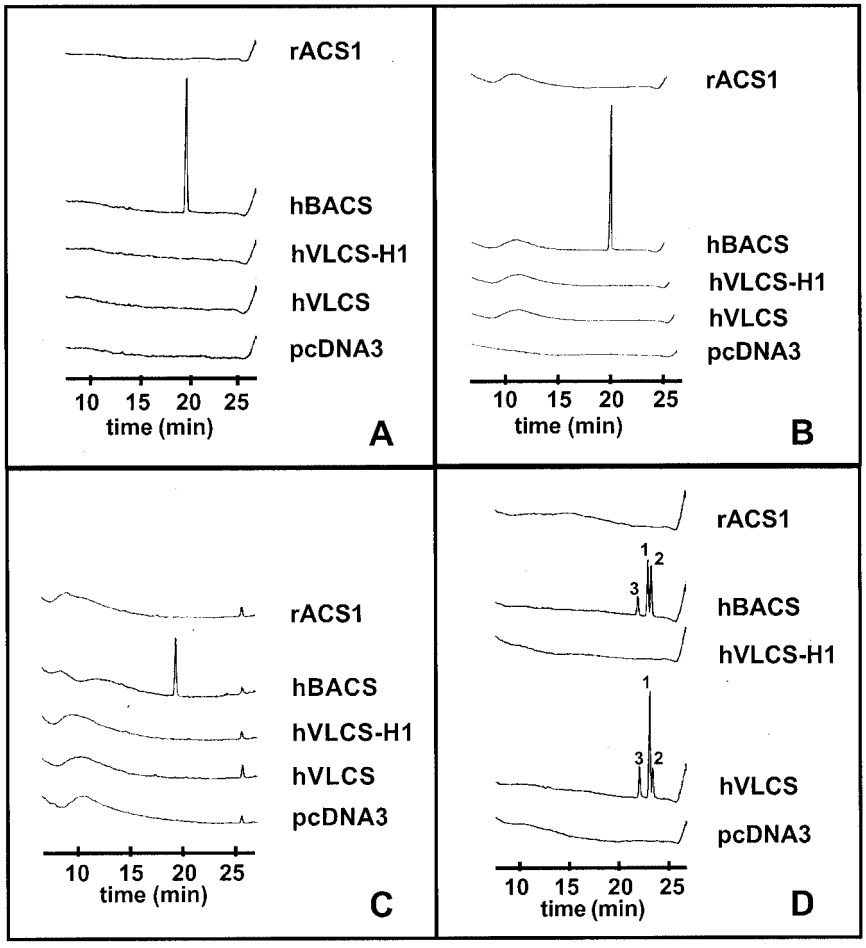

FIG. 1. **Activation of bile acids and THCA by hVLCS and hBACS.** COS-1 cells were transfected with full-length cDNA encoding hVLCS, hVLCS-H1, hBACS, or rACS1 or with the vector (pcDNA3) alone; harvested 72 h post-transfection; disrupted by freeze/thaw; and incubated for 20 min at 37 °C with ATP, $MgCl_2$, CoA, and the indicated substrate at 20 μM. Products were analyzed by reverse-phase HPLC as described under "Experimental Procedures." Shown is the activation of chenodeoxycholate (*A*), deoxycholate (*B*), lithocholate (*C*), and THCA (*D*). In *D*, peak 1 is (25*S*)-THCA-CoA, peak 2 is (25*R*)-THCA-CoA, and peak 3 is Δ24-THCA-CoA. Two to three independent transfection experiments yielded identical results.

(Fisher), fixed for 30 min with 4% paraformaldehyde in phosphate-buffered saline, and acetylated for 10 min in 0.25% acetic anhydride in 0.1 M triethanolamine. After 8 h of prehybridization in 50% formamide containing 5× Denhardt's solution (Sigma), 5× SSC, and 0.25 mg/ml yeast tRNA (Invitrogen), slices were hybridized in the same buffer containing digoxigenin-labeled probes (200 ng/ml) for 16 h at 60 °C. The slides were washed under high-stringency conditions (5× SSC in 50% formamide for 5 min at 59 °C, 2× SSC for 1 min at 59 °C, 0.2× SSC for 30 min at 65 °C, and 0.2% SSC for 5 min at room temperature). After a 1-h incubation in blocking reagent (Roche Molecular Biochemicals), slices were incubated for 1.5 h with alkaline phosphatase-conjugated anti-digoxigenin antibody (Roche Molecular Biochemicals). Color development with nitro blue tetrazolium and 5-bromo-4-chloro-3-indolyl phosphate was carried out for 16 h.

RESULTS

hBACS Catalyzes Activation of Primary and Secondary Bile Acids—We previously showed that when expressed in COS-1 cells, hBACS (formerly called hVLCS-H2, a member of the VLCS/fatty acid transport protein family of acyl-CoA synthetases) catalyzes the activation of cholic acid to its CoA derivative (7). This observation was consistent with the tissue (liver) and subcellular (endoplasmic reticulum) distribution of this protein (17, 18). We also reported that hBACS weakly activates the very long-chain fatty acid lignoceric acid ($C_{24:0}$; 20–40% of the activity measured with cholate) and was not able to activate the long-chain fatty acid palmitic acid ($C_{16:0}$) (7, 12). To determine whether the other human primary bile acid, chenodeoxycholic acid, and the secondary bile acids deoxycholic acid and lithocholic acid are also substrates for hBACS, we incubated these compounds with ATP, $MgCl_2$, CoA and freeze/thaw-disrupted COS-1 cells expressing this or related proteins. The products were separated by HPLC as previously described (7). When chenodeoxycholate was the substrate, a product with a retention time of 20.3 min was detected in cells expressing hBACS (Fig. 1*A*). No product was detected in cells transfected with hVLCS, hVLCS-H1, rat liver long-chain acyl-CoA synthetase-1 (rACS1), or the vector (pcDNA3) alone (Fig. 1*A*). We had previously reported that no product is formed in the absence of ATP, CoA, or the bile acid substrate (7) (data not shown). To substantiate the results of the HPLC-based assay, we incubated COS-1 cells expressing hBACS and related proteins with radiolabeled chenodeoxycholate (Fig. 2*A*). Again, only cells expressing hBACS were capable of catalyzing chenodeoxycholate activation. Thus, we conclude that chenodeoxycholate is also a substrate for hBACS.

Similar results were obtained using the HPLC-based assay when the secondary bile acids deoxycholate (Fig. 1*B*) and lithocholate (Fig. 1*C*) were substrates for activation by hBACS. The putative products deoxycholoyl-CoA and lithocholoyl-CoA eluted at 21.7 and 19.7 min, respectively. No product was detected with either substrate in cells expressing hVLCS, hVLCS-H1, or rACS1, consistent with the hypothesis that the liver-specific hBACS is a bile acyl-CoA synthetase capable of activating both primary and secondary bile acids.

Both hVLCS and hBACS Activate the Bile Acid Precursor THCA—Based on the above observations, we predicted that the C_{27} precursor of cholic acid (THCA) would be activated to its CoA derivative by hBACS, but not by the other hVLCSs or rACS1. When THCA was incubated with ATP, $MgCl_2$, CoA, and COS-1 cells expressing hBACS, three product peaks were seen on the HPLC tracing (Fig. 1*D*). The substrate used is a racemic mixture of (25*S*)- and (25*R*)-THCA stereoisomers. It was previously shown that the physiologic isomer ((25*S*)-THCA) elutes slightly earlier than the non-physiologic isomer ((25*R*)-THCA)

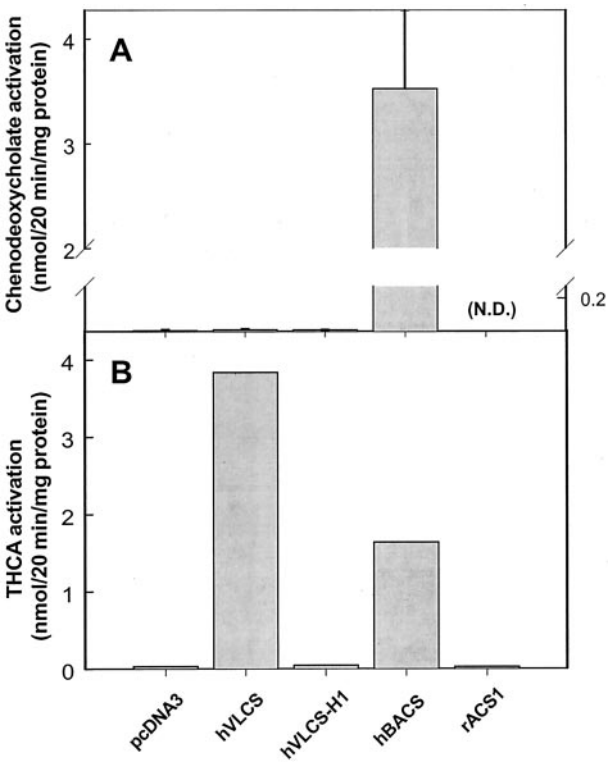

FIG. 2. **Activation of radiolabeled chenodeoxycholate and THCA by hVLCS and hBACS.** COS-1 cells expressing hVLCS, hVLCS-H1, hBACS, rACS1, or the vector alone were incubated with ATP, $MgCl_2$, CoA, and 20 μM [1-^{14}C]chenodeoxycholate (*A*) or 20 μM [26-^{14}C]THCA (*B*). After 20 min, labeled CoA derivatives were extracted from the reaction mixture, and the radioactivity was determined as described under "Experimental Procedures." The results in *A* are the means ± S.E. from three separate transfection experiments. Because of the limited availability of [26-^{14}C]THCA, the results in *B* are the mean of two separate transfections. *N.D.*, not determined.

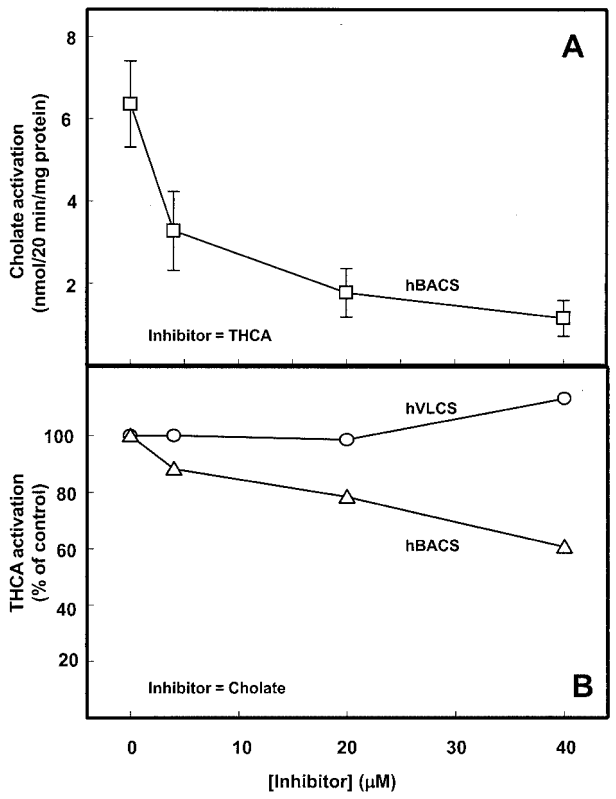

FIG. 3. **Inhibition of hVLCS and hBACS by cholate and THCA.** *A*, THCA inhibition of [1-^{14}C]cholate activation by hBACS. COS-1 cells expressing hBACS were incubated with 20 μM [1-^{14}C]cholate and the indicated concentration of unlabeled THCA. The production of labeled choloyl-CoA was quantitated as described under "Experimental Procedures." The results are the means ± S.E. from three separate transfection experiments. *B*, cholate inhibition of THCA activation by hVLCS or hBACS. COS-1 cells expressing hVLCS (○) or hBACS (△) were incubated with 20 μM THCA and the indicated concentration of cholate. Production of (25*S*)-THCA-CoA was quantitated by reverse-phase HPLC as described under "Experimental Procedures." The results are expressed as percent of the control (no cholate) and are the means of two separate transfections.

in a similar HPLC system (19). Thus, we have provisionally designated peak 1 (23.4 min) as (25*S*)-THCA and peak 2 (23.7 min) as (25*R*)-THCA. Peak 3 had a retention time (22.3 min) identical to that of 3α,7α,12α-trihydroxy-5β-cholest-24-en-26-oyl-CoA (see "Experimental Procedures") (data not shown). This compound is the product formed by the action of peroxisomal branched-chain acyl-CoA oxidase on (25*S*)-THCA and accumulates when fibroblasts from children with mutations in the 3-hydroxyacyl-CoA dehydrogenase domain of peroxisomal D-bifunctional protein are incubated with 24-OH-THCA (15).

Similar to the situation with primary and secondary bile acids, no product was detected when THCA was incubated with COS-1 cells expressing hVLCS-H1, rACS1, or the vector alone (Fig. 1*D*). In contrast, cells expressing hVLCS (which were not capable of activating the bile acids) yielded the same three product peaks as did cells expressing hBACS (Fig. 1*D*). This observation suggests that both hVLCS and hBACS are capable of activating THCA for its subsequent conversion to cholate.

The ability of hVLCS and hBACS to activate THCA was confirmed by radiochemical assay using [26-^{14}C]THCA as substrate. COS-1 cells expressing either hVLCS or hBACS exhibited THCA-CoA synthetase activity (Fig. 2*B*). COS-1 cells transfected with the vector (pcDNA3) alone, hVLCS-H1, or rACS1 were unable to activate [26-^{14}C]THCA (Fig. 2*B*).

THCA Inhibits hBACS-catalyzed Activation of Cholate—To elucidate the role(s) of hVLCS and hBACS in bile acid metabolism, we first investigated the ability of the biosynthetic precursor of cholate (THCA) to inhibit cholate activation. We incubated COS-1 cells expressing hBACS with radiolabeled cholate in the presence of increasing concentrations of THCA. A concentration of THCA (4 μM) that was 20% of the cholate concentration (20 μM) reduced cholate activation by nearly half (Fig. 3*A*). When THCA was present at the same (20 μM) and at double (40 μM) the cholate concentration, we observed 72 and 82% inhibition, respectively (Fig. 3*A*).

Cholate Inhibits Activation of THCA by hBACS, but Not by hVLCS—Because cholate is a substrate for hBACS, but not for hVLCS, we next examined the effect of unlabeled cholate on THCA activation by these two enzymes. When COS-1 cells expressing hBACS were incubated with 20 μM THCA, formation of (25*S*)-THCA-CoA was reduced by 11, 21, and 39% when 4, 20, and 40 μM cholate, respectively, were present in the assay (Fig. 3*B*). In contrast, with COS-1 cells expressing hVLCS, an enzyme that does not activate cholate, there was no apparent cholate inhibition of THCA activation (Fig. 3*B*).

Kinetic Studies of Cholate and Palmitate Activation—Kinetic studies were performed to establish further that hVLCS does not activate bile acids and that hBACS does not activate long-chain fatty acids. COS-1 cells expressing hBACS exhibited normal Michaelis-Menten kinetics when cholate was the substrate (Fig. 4*A*); cells transfected with the vector alone had no activity with this substrate (data not shown). Under these conditions, the K_m of hBACS for cholate was 2.8 μM, and the V_{max} was 3.8 nmol/20 min/mg of COS cell protein, as determined by nonlinear regression analysis. Similar experiments were performed using the substrate palmitic acid ($C_{16:0}$), a

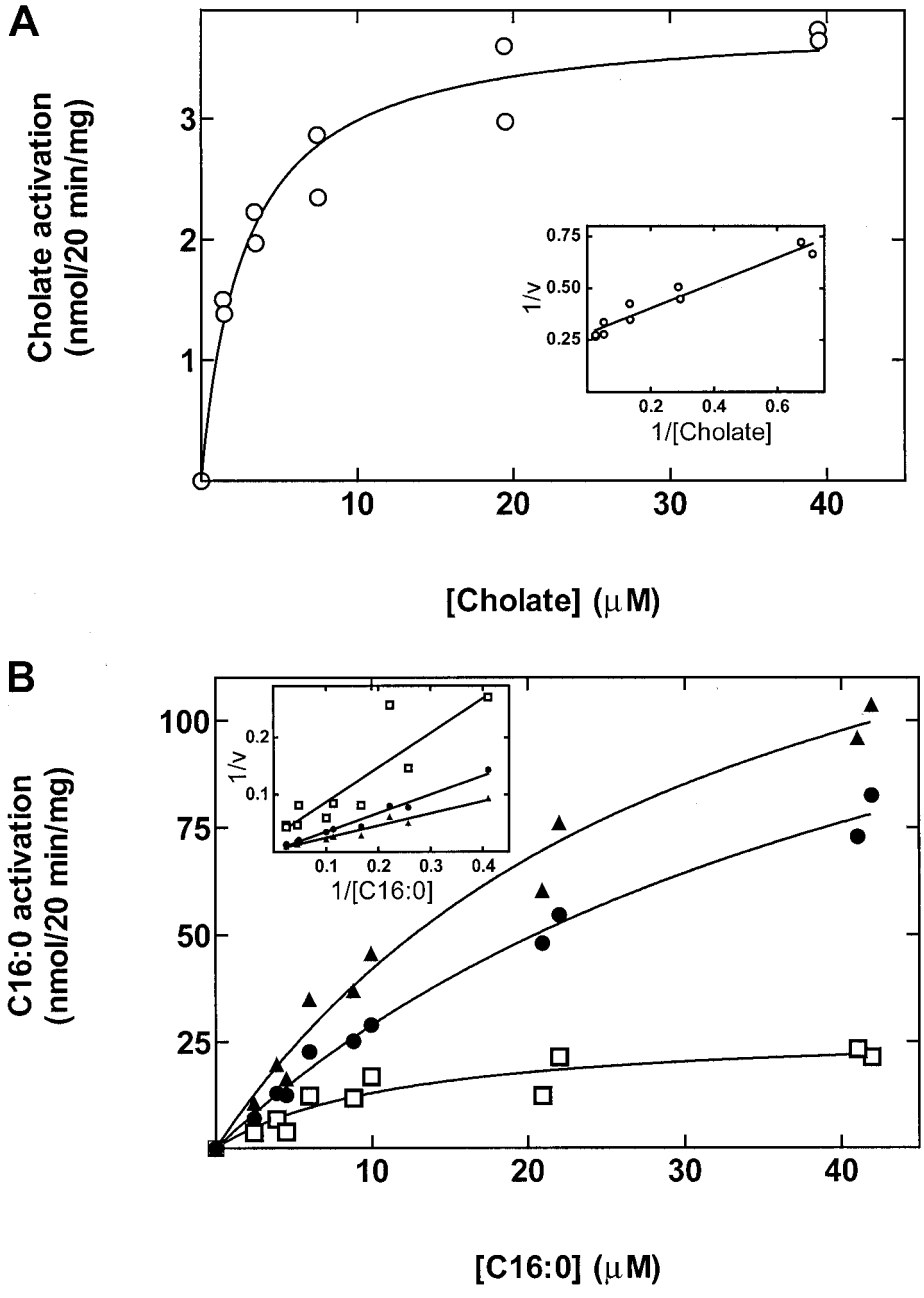

FIG. 4. **Kinetic analysis.** COS-1 cells expressing pcDNA3, hBACS, or hVLCS were assayed for their ability to activate the bile acid cholate (a preferred substrate for hBACS) or the long-chain fatty acid palmitate ($C_{16:0}$, a preferred substrate for hVLCS). *A*, [1-^{14}C]cholate activation by hBACS exhibited typical Michaelis-Menten kinetics. A Lineweaver-Burk double-reciprocal plot is shown in the *inset*. Replicate data from two independent transfections are plotted on the same curve. K_m and V_{max} were calculated by nonlinear regression analysis using GraphPAD Prism Version 3.02 for Windows. [1-^{14}C]Cholate activation by hVLCS was not detectable at any cholate concentration tested (data not shown). *B*, [1-^{14}C]palmitate activation in vector-transfected COS-1 cells (●) or cells expressing hVLCS (▲) exhibited apparently normal Michaelis-Menten kinetics. The contribution of hVLCS to the total $C_{16:0}$ activation was estimated by subtraction (□). A Lineweaver-Burk double-reciprocal plot is shown in the *inset*. Replicate data from two independent transfections are plotted on the same curve and were analyzed by GraphPAD Prism software. No $C_{16:0}$-CoA synthetase activity in hBACS-expressing cells that was statistically significantly different from that in vector-transfected cells was measured.

long-chain fatty acid that is the preferred substrate for hVLCS (8). Kinetic analysis is complicated by the fact that untransfected and vector-transfected COS-1 cells contain several endogenous acyl-CoA synthetases that can activate $C_{16:0}$ (see Fig. 4*B*); thus, endogenous activity must be subtracted from that of hBACS-transfected cells. At each of five $C_{16:0}$ concentrations tested (range of 2.5–40 μM), there was no statistically significant increase in $C_{16:0}$ activation by hBACS-transfected cells compared with pcDNA3-transfected cells ($p \geq 0.1$, $n = 3$; data not shown). It is therefore unlikely that $C_{16:0}$ is activated to a significant degree by hBACS *in vivo*.

The kinetics of $C_{16:0}$ and cholate activation by COS-1 cells expressing hVLCS were also examined. When $C_{16:0}$ was the substrate, both pcDNA3- and hVLCS-transfected COS-1 cells exhibited apparently normal Michaelis-Menten kinetics (Fig. 4*B*). Nonlinear regression analysis revealed a K_m of 48 μM and a V_{max} of 167 nmol/20 min/mg of COS cell protein for vector-transfected cells and a K_m of 32 μM and a V_{max} of 175 nmol/20 min/mg of COS cell protein for cells expressing hVLCS. The contribution of hVLCS to the overall $C_{16:0}$-CoA synthetase activity was estimated by subtraction (Fig. 4*B*), and a K_m of 12 μM and a V_{max} of 28 nmol/20 min/mg of COS cell protein were calculated. It must be emphasized that these derived values are, at best, crude estimates. In our previous study (7), we found that neither vector-transfected nor hVLCS-transfected COS-1 cells activate 20 μM cholate to its CoA derivative. We now report that no detectable activation was observed at any of five concentrations of cholate tested (range of 2.5–40 μM) (data not shown).

Hepatic Organization of VLCS- and BACS-expressing Cells—We hypothesize that the primary metabolic role of hBACS is bile acid activation. On the other hand, although hVLCS may play a role in bile acid synthesis from THCA, this enzyme can activate a wide variety of substrates, including long-, very long-, and branched-chain fatty acids (7, 8). If these two synthetases have different functions, the intrahepatic localization of cells expressing them might differ. We used *in situ* hybridization to address this question in mouse liver. Using an

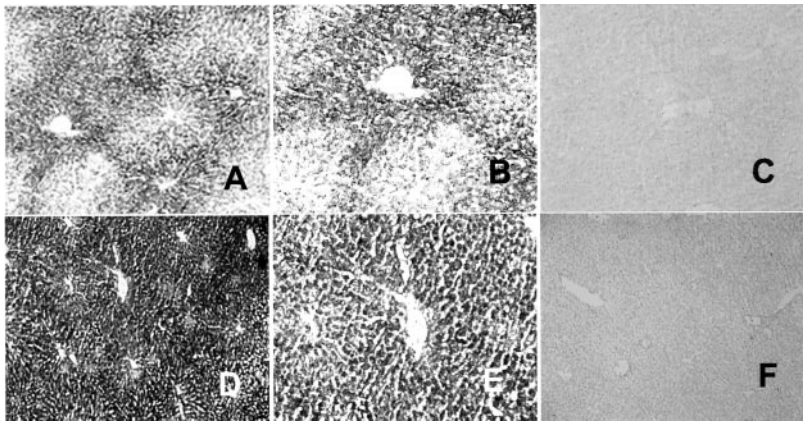

FIG. 5. **Hepatic expression pattern of VLCS and BACS.** Full-length cDNA encoding the murine homolog of either VLCS or BACS as template was used to prepare sense and antisense RNA probes, which were then hybridized with 8-μm frozen sections of normal adult mouse liver as described under "Experimental Procedures." *A* and *B*, BACS antisense probe; *C*, BACS sense probe; *D* and *E*, VLCS antisense probe; *F*, VLCS sense probe. Magnification ×100 (*A*, *C*, *D*, and *F*) and ×200 (*B* and *E*).

antisense RNA probe synthesized from cDNA encoding the murine ortholog of hVLCS, we found that hepatocytes uniformly expressed this enzyme (Fig. 5, *D* and *E*). In contrast, hepatocytes expressing the murine homolog of hBACS mainly had a periportal distribution (Fig. 5, *A* and *B*). These observations are consistent with the differing proposed roles of the two acyl-CoA synthetases in bile acid and fatty acid metabolism.

Topographic Orientation of hVLCS and hBACS Expressed in COS-1 Cells—We previously reported that although hBACS is primarily a microsomal enzyme, hVLCS is localized to both peroxisomes and the endoplasmic reticulum (8, 20). Other laboratories have reported that activation of both bile acids (17, 18, 21) and the bile acid precursors DHCA and THCA (22) occurs in microsomes. The fact that hBACS activates both bile acids and THCA is consistent with these reports. Our observation that hVLCS, with its dual subcellular location, can activate THCA, but not bile acids, raised questions about the precise role(s) of hVLCS and hBACS in bile acid synthesis.

An initial approach to answer this question was to examine the topographic orientation of hVLCS and hBACS in the endoplasmic reticulum membrane. For these studies, epitope tags were placed at either end of the expressed proteins. Full-length hVLCS cDNA clones incorporating an in-frame *myc* epitope at the N and C termini were constructed as outlined under "Experimental Procedures." Similar *myc*-tagged constructs of hBACS were prepared. COS-1 cells expressing these cDNAs were examined by indirect immunofluorescence using anti-*myc* antibody to determine the orientation of the expressed protein. We previously reported that when COS-1 cells expressing hVLCS are permeabilized with Triton X-100, the protein is detected primarily in the endoplasmic reticulum, whereas the endogenous protein is also detected in peroxisomes (8, 20). COS-1 cells transfected with either N-*myc*-hVLCS (Fig. 6*A*) or C-*myc*-hVLCS (Fig. 6*E*) also had a staining pattern consistent with expression in the endoplasmic reticulum. The location was confirmed by colocalization of immunofluorescence of hVLCS with that of the endoplasmic reticulum luminal resident protein calreticulin (Fig. 6, *B* and *F*). Also as reported previously (12), an endoplasmic reticulum N-*myc*-hBACS staining pattern was observed in Triton X-100-permeabilized COS-1 cells expressing this protein (Fig. 6*I*). Cells expressing C-*myc*-hBACS had an identical immunostaining pattern (Fig. 6*M*).

Permeabilization of cells with digitonin rather than Triton X-100 yielded a somewhat different result. The C-*myc*-hVLCS protein was detected in digitonin-permeabilized COS-1 cells transfected with its cDNA (Fig. 6*G*), but N-*myc*-hVLCS was not visualized (Fig. 6*C*). Under the conditions utilized, the luminal protein calreticulin could not be detected (Fig. 6, *D* and *H*). These data indicate that although the C terminus of hVLCS faces the cytoplasm, the N terminus faces the lumen of the

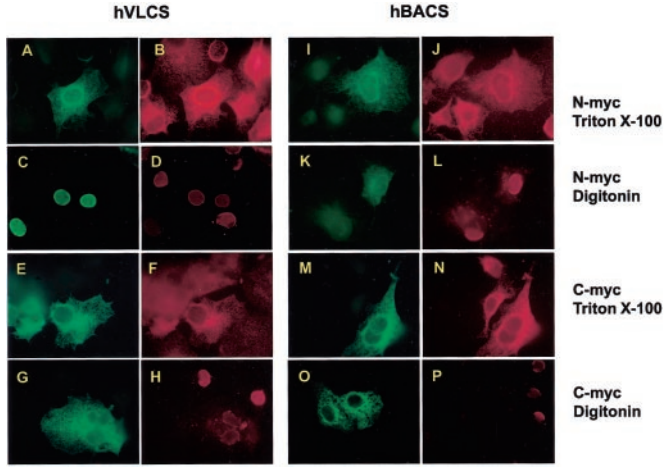

FIG. 6. **Topographic orientation of hVLCS and hBACS in endoplasmic reticulum membranes.** COS-1 cells were transfected with full-length hVLCS or hBACS constructs containing the c-*myc* epitope in-frame at either the N or C terminus of the protein. Three days following transfection, cells were fixed and permeabilized with either Triton X-100 (exposing antigens facing both the cytoplasm and the endoplasmic reticulum lumen) or digitonin (exposing antigens facing the cytoplasm only). Double-label indirect immunofluorescence analyses using antibodies specific for the c-*myc* epitope and the endoplasmic reticulum luminal resident protein calreticulin were performed as described under "Experimental Procedures." The anti-*myc* antibody was detected by a fluorescein-conjugated secondary antibody (*green*), whereas the anti-calreticulin antibody was detected by a lissamine rhodamine-conjugated secondary antibody (*red*). *A–H*, cells expressing hVLCS; *I–P*, cells expressing hBACS. The position of the epitope tag (N-*versus* C-terminal) and the permeabilization method (Triton X-100 *versus* digitonin) are indicated on the *right*. Both C-*myc*-hBACS and N-*myc*-hBACS were enzymatically active when expressed in COS-1 cells (~50 and ~20% of untagged hBACS activity, respectively). N-*myc*-hVLCS and untagged hVLCS activated palmitic acid equally well, but the activity of C-*myc*-hVLCS was <20% than that of hVLCS. However, the results of topographic experiments with hVLCS (untagged and enzymatically active)-transfected cells and an antibody raised against the C terminus of this protein gave results identical to those obtained with C-*myc*-hVLCS and anti-*myc* antibody (7) (data not shown).

endoplasmic reticulum. We previously reported that the C terminus of endogenous hVLCS is oriented toward the peroxisomal matrix and not the cytoplasm (20). In contrast, both the N-*myc*-hBACS (Fig. 6*K*) and C-*myc*-hBACS (Fig. 6*O*) proteins could be detected in digitonin-permeabilized cells (compare with calreticulin) (Fig. 6, *L* and *P*). These data suggest that hBACS may preferentially act on substrates present in the cytoplasm.

DISCUSSION

The synthesis of bile acids from cholesterol, conjugation with amino acids, secretion into the bile and subsequently into the

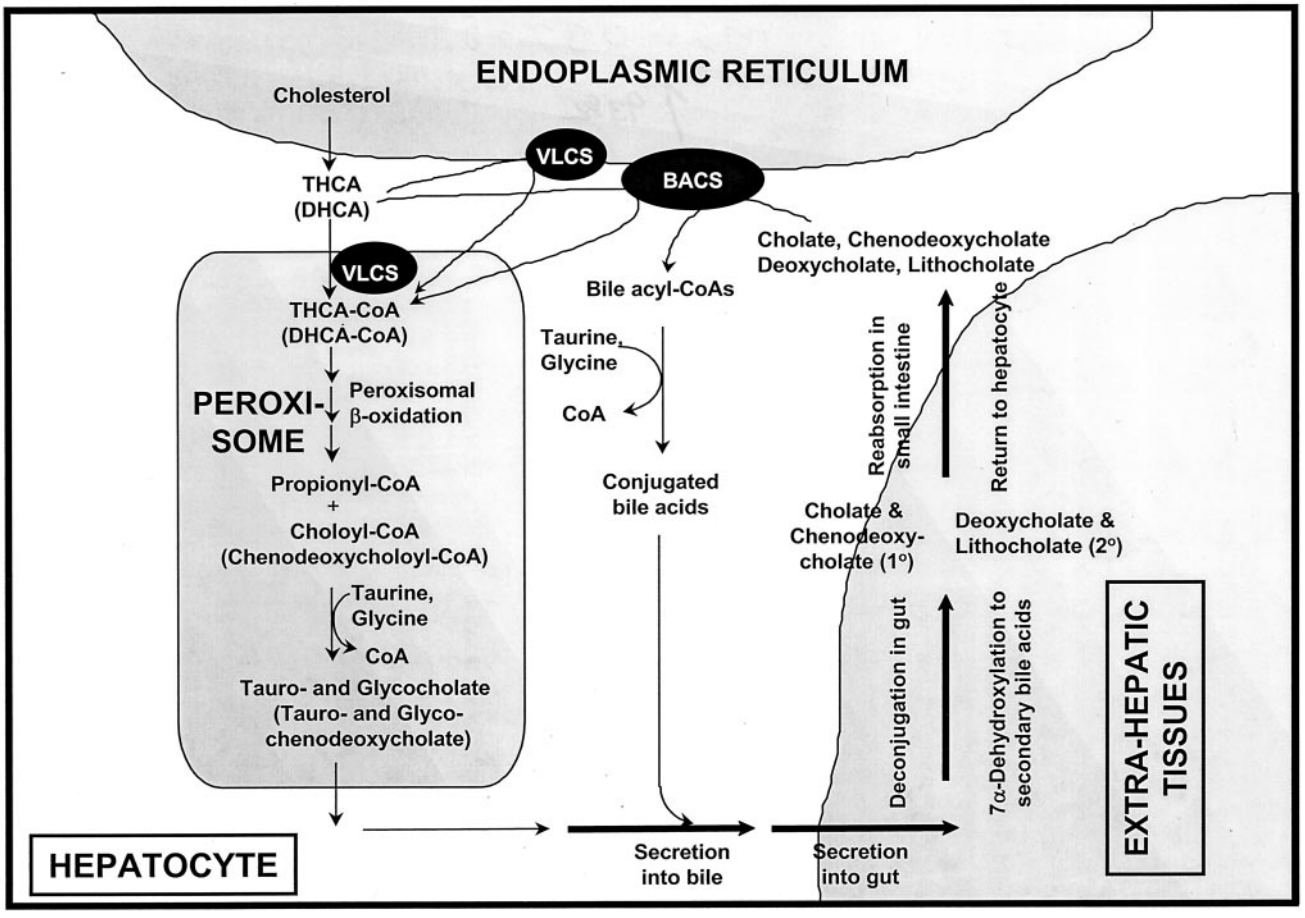

FIG. 7. **Proposed roles of VLCS and BACS in bile acid metabolism.**

intestinal tract, reabsorption from the intestine, and reutilization require the integrated activity of multiple enzymes, organelles, and tissues. At two points in the hepatic phase of bile acid metabolism, activation of the carboxylic acid side chain of the steroid to a CoA derivative is required. First, in the pathway of *de novo* synthesis from cholesterol, the C_{27} precursors of cholate and chenodeoxycholate (THCA and DHCA, respectively) must be converted to THCA-CoA and DHCA-CoA for cleavage of three carbons from the side chain to occur. Second, to conjugate the C_{24} bile acids cholate and chenodeoxycholate to glycine or taurine, their carboxylic acid side chains must first be activated to the corresponding CoA derivatives. The studies reported here begin to address the nature of the acyl-CoA synthetases that are involved in these two aspects of bile acid metabolism.

Based on the biochemical and morphological data presented here and our previous findings (7), we have developed a working hypothesis regarding the role(s) of hVLCS and hBACS in bile acid metabolism (Fig. 7). Conversion of cholesterol to THCA and DHCA requires several enzymatic steps that take place in the endoplasmic reticulum, cytosol, and mitochondria (1, 2). Activation of THCA and DHCA, precursors of cholic acid and chenodeoxycholic acid, respectively, could be catalyzed by either hVLCS or hBACS in the endoplasmic reticulum or by hVLCS in peroxisomes. Once inside peroxisomes, the side chains of THCA-CoA and DHCA-CoA are shortened by three carbons via β-oxidation, yielding choloyl-CoA and chenodeoxycholoyl-CoA, respectively. The peroxisomal enzyme bile acyl-CoA:amino-acid *N*-acyltransferase (23) then catalyzes the formation of the glycine and taurine conjugates of cholic acid and chenodeoxycholic acid. Exiting the peroxisome, the conjugated bile acids are secreted into bile canaliculi and eventually reach the small intestine. Although a large proportion of the conjugated bile acids remain intact, a small quantity undergoes conversion in the bowel. Intestinal flora catalyze both deconjugation and dehydroxylation reactions (1, 2). 7α-Dehydroxylation of cholate and chenodeoxycholate yields the secondary bile acids deoxycholate and lithocholate, respectively. Intestinal metabolism thus yields a mixture of primary and secondary bile acids that includes both conjugated and free acids. Reabsorption of free bile acids occurs by passive diffusion throughout the small bowel (1, 24). When these free acids reach the liver via the portal circulation, they must be reactivated and then conjugated before they are returned to the bile. hBACS is uniquely positioned in the endoplasmic reticulum membrane to catalyze the reactivation reaction. Bile acyl-CoA:amino-acid *N*-acyltransferase is found in the cytoplasm as well as the peroxisome (17, 25). Following re-conjugation in the cytoplasm, primary and secondary bile acids can be secreted into the bile for reutilization. This hypothesis is consistent with that recently proposed by Solaas *et al.* (25), who investigated bile acyl-CoA:amino-acid *N*-acyltransferase in human liver.

Using subcellular fractions from rat liver, other investigators have shown that activation of THCA to its CoA derivative occurs primarily in microsomes (22, 25). Our data indicate that both hVLCS and hBACS are capable of activating THCA and that both enzymes are found in the endoplasmic reticulum. Because hVLCS is also found in peroxisomes (8, 20), it is not clear why Schepers *et al.* (22) and Solaas *et al.* (25) did not detect significant THCA activation in peroxisome-enriched liver fractions. Activation of THCA in peroxisomes rather than in microsomes is a more attractive hypothesis because CoA derivatives generally do not

cross biological membranes. hVLCS is oriented in the peroxisomal membrane facing the matrix (20, 26), and activation of THCA would use intraperoxisomal CoA-SH. Amidation of the β-oxidation product, choloyl-CoA, by peroxisomal bile acyl-CoA:amino-acid *N*-acyltransferase would regenerate free CoA-SH inside the organelle.

Alternatively, if activation of THCA takes place solely in the endoplasmic reticulum, the CoA-SH balance must somehow be maintained. A possible mechanism for maintaining a constant intraperoxisomal CoA-SH pool is one in which THCA-CoA entering the organelle is coupled to CoA-SH exiting. However, it is not clear at this time how either THCA or THCA-CoA enters peroxisomes. Furthermore, it remains to be determined whether the THCA activation reaction is catalyzed primarily by VLCS or by BACS, if this process does not occur in peroxisomes. Data reported by Schepers *et al.* (22) on pH dependence and Triton X-100 sensitivity indicate that in rat liver microsomes, the enzyme catalyzing THCA activation is distinct from that catalyzing cholate activation. This suggests that VLCS and not BACS might be the primary enzyme that activates THCA. On the other hand, Wheeler *et al.* (27) purified a bile acid:CoA ligase from rat liver (most likely rat BACS) that activated both chenodeoxycholate and THCA. We plan to address this issue in future studies by investigating THCA activation in subcellular fractions prepared from livers of mice in which the VLCS gene has been disrupted.[2]

The data presented here suggest that hVLCS activates THCA more robustly than does hBACS and is not sensitive to inhibition by cholate. These results are consistent with the notion that hVLCS has a diverse role in metabolism, activating both fatty acids and THCA. In contrast, hBACS showed a greater preference for bile acids and their precursors as substrates, suggesting a more limited role for this enzyme (7, 12). THCA inhibition of choloyl-CoA synthesis was stronger than cholate inhibition of THCA-CoA synthesis in hBACS-transfected cells. These data are consistent with those reported by Schepers *et al.* (22) for rat liver microsomes.

The peroxisomal pathway for chain shortening of the C_{27} compounds THCA-CoA and DHCA-CoA to C_{24} bile acids by β-oxidation is now well established (3). In humans, the first step is catalyzed by branched-chain acyl-CoA oxidase, the same enzyme that oxidizes α-methyl-branched fatty acids such as pristanic acid (28). In rodents, distinct enzymes carry out these two processes (29). D-bifunctional protein catalyzes the second (enoyl-CoA hydratase) and third (hydroxyacyl-CoA dehydrogenase) activities (30). The thiolase associated with the 58-kDa protein sterol carrier protein X is thought to carry out the final reaction, thiolytic cleavage and release of propionyl-CoA (31). It is noteworthy that the C_{24} products of the thiolase reaction are the CoA derivatives of cholic acid and chenodeoxycholic acid and not the free acids. Furthermore, bile acyl-CoA:amino-acid *N*-acyltransferase, the conjugating enzyme, contains a peroxisomal targeting signal and can be detected in this organelle (23). Thus, peroxisomes possess the complete enzymatic machinery required to convert THCA and DHCA into conjugated bile acids.

In situ hybridization studies are consistent with the proposed roles of VLCS and BACS in bile acid and fatty acid metabolism. Hepatic lipogenic enzymes appear to have a more perivenous distribution (32, 33), whereas the rate-limiting step in bile acid synthesis, cholesterol 7α-hydroxylase, is found mainly in periportal hepatocytes (34). Expression of hBACS was also found to have a more periportal distribution. The enterohepatic circulation returns bile acids to the liver via the portal vein; thus, hBACS is well positioned to efficiently "scavenge" these bile acids, reactivating them for recycling. In contrast, hVLCS, which robustly activates fatty acids as well as THCA, had a more uniform distribution throughout the liver acinus.

The topographic orientation of hBACS, in which both the C and N termini face the cytoplasm, also makes it well suited for its proposed role in reactivation of bile acids returning to the hepatocytes via the enterohepatic circulation. Analysis of the hBACS amino acid sequence by the PHDhtm algorithm revealed that the protein contains no unequivocal transmembrane-spanning domains (35). The orientation of hVLCS in the endoplasmic reticulum membrane, with the N terminus facing the lumen and the C terminus facing the cytoplasm, is consistent with the model proposed by Smith *et al.* (26). These authors suggested that VLCS is an integral membrane protein in microsomes. Schepers *et al.* (22) were unable to release THCA-CoA synthetase activity from microsomes using high salt alone, consistent with the notion that VLCS and not BACS is primarily responsible for this synthetase activity.

In summary, in this report, we have described the ability of two members of the VLCS/fatty acid transport protein family to activate bile acids and their precursors. Based on these data, we presented a working hypothesis regarding the roles of these enzymes in bile acid metabolism. Solaas *et al.* (25) recently hypothesized that the peroxisomal conversion of THCA to choloyl-CoA is the rate-limiting step in production of conjugated bile acids via *de novo* synthesis. They further proposed that the rate-limiting step in the reutilization of bile acids returning to the liver via the enterohepatic circulation is the reactivation step (25). Future studies will enable us to test these hypotheses.

Acknowledgments—We thank Zhenzhen Jia, Gloria Cha, and Anisa Chaudhry for expert technical assistance. Fibroblasts from patients with mutations in the enoyl hydratase domain of peroxisomal D-bifunctional protein were obtained through the Mental Retardation Research Center of the Kennedy Krieger Institute.

REFERENCES

1. Setchell, K. D. R., and O'Connell, N. C. (2001) in *Liver Disease in Children* (Suchy, F. J., Sokol, R. J., and Balistreri, W. F., eds) 2nd Ed., pp. 701–733, Lippincott Williams & Wilkins, Philadelphia
2. Vlahcevic, Z. R., Pandak, W. M., and Stravitz, R. T. (1999) *Gastroenterol. Clin. North Am.* **28,** 1–25
3. Wanders, R. J. A., Barth, P. C., and Heymans, H. S. A. (2001) in *The Metabolic & Molecular Bases of Inherited Disease* (Scriver, C. R., Beaudet, A. L., Sly, W. S., and Valle, D., eds) 8th Ed., pp. 3219–3256, McGraw-Hill Book Co., New York
4. Kase, F., Bjorkhem, I., and Pedersen, J. I. (1983) *J. Lipid Res.* **24,** 1560–1567
5. Hofmann, A. F. (1994) in *The Liver: Biology and Pathobiology* (Arias, A. M., Boyer, J. L., Fausto, N., Jakoby, W. B., Schachter, D. A., and Shafritz, D. A., eds) 3rd Ed., pp. 677–718, Raven Press, New York
6. Carey, M. C., and Duane, W. C. (1994) in *The Liver: Biology and Pathobiology* (Arias, A. M., Boyer, J. L., Fausto, N., Jakoby, W. B., Schachter, D. A., and Shafritz, D. A., eds) 3rd Ed., pp. 719–767, Raven Press, New York
7. Steinberg, S. J., Mihalik, S. J., Kim, D. G., Cuebas, D. A., and Watkins, P. A. (2000) *J. Biol. Chem.* **275,** 15605–15608
8. Steinberg, S. J., Wang, S. J., Kim, D. G., Mihalik, S. J., and Watkins, P. A. (1999) *Biochem. Biophys. Res. Commun.* **257,** 615–621
9. Lowry, O. H., Rosebrough, N. J., Farr, A. L., and Randall, R. J. (1951) *J. Biol. Chem.* **193,** 265–275
10. Xu, R. F., and Cuebas, D. A. (1996) *Biochem. Biophys. Res. Commun.* **221,** 271–278
11. Tserng, K. Y., and Klein, P. D. (1977) *J. Lipid Res.* **18,** 400–403
12. Steinberg, S. J., Wang, S. J., McGuinness, M. C., and Watkins, P. A. (1999) *Mol. Genet. Metab.* **68,** 32–42
13. Uchiyama, A., Aoyama, T., Kamijo, K., Uchida, Y., Kondo, M., Orii, T., and Hashimoto, T. (1996) *J. Biol. Chem.* **271,** 30360–30365
14. Watkins, P. A., Gould, S. J., Smith, M. A., Braiterman, L. T., Wei, H.-M., Kok, F., Moser, A. B., Moser, H. W., and Smith, K. D. (1995) *Am. J. Hum. Genet.* **57,** 292–301
15. van Grunsven, E. G., van Berkel, E., Ijlst, L., Vreken, P., de Klerk, J. B., Adamski, J., Lemonde, H., Clayton, P. T., Cuebas, D. A., and Wanders, R. J. (1998) *Proc. Natl. Acad. Sci. U. S. A.* **95,** 2128–2133
16. Giger, R. J., Wolfer, D. P., De Wit, G. M., and Verhaagen, J. (1996) *J. Comp. Neurol.* **375,** 378–392
17. Killenberg, P. G. (1978) *J. Lipid Res.* **19,** 24–31
18. Polokoff, M. A., and Bell, R. M. (1977) *J. Biol. Chem.* **252,** 1167–1171

[2] A. K. Heinzer, P. A. Watkins, and K. D. Smith, unpublished data.

19. Kurosawa, T., Sato, M., Inoue, K., Yoshimura, T., Tohma, M., Jiang, L. L., and Hashimoto, T. (1998) *Anal. Chim. Acta* **365,** 249–257
20. Steinberg, S. J., Kemp, S., Braiterman, L. T., and Watkins, P. A. (1999) *Ann. Neurol.* **46,** 409–412
21. Lim, W. C., and Jordan, T. W. (1981) *Biochem. J.* **197,** 611–618
22. Schepers, L., Casteels, M., Verheyden, K., Parmentier, G., Asselberghs, S., Eyssen, H. J., and Mannaerts, G. P. (1989) *Biochem. J.* **257,** 221–229
23. Kase, B. F., and Bjorkhem, I. (1989) *J. Biol. Chem.* **264,** 9220–9223
24. Bahar, R. J., and Stolz, A. (1999) *Gastroenterol. Clin. North Am.* **28,** 27–58
25. Solaas, K., Ulvestad, A., Soreide, O., and Kase, B. F. (2000) *J. Lipid Res.* **41,** 1154–1162
26. Smith, B. T., Sengupta, T. K., and Singh, I. (2000) *Exp. Cell Res.* **254,** 309–320
27. Wheeler, J. B., Shaw, D. R., and Barnes, S. (1997) *Arch. Biochem. Biophys.* **348,** 15–24
28. Vanhove, G. F., Van Veldhoven, P. P., Fransen, M., Denis, S., Eyssen, H. J., Wanders, R. J. A., and Mannaerts, G. P. (1993) *J. Biol. Chem.* **268,** 10335–10344
29. Van Veldhoven, P. P., Vanhove, G., Asselberghs, S., Eyssen, H. J., and Mannaerts, G. P. (1992) *J. Biol. Chem.* **267,** 20065–20074
30. Dieuaide-Noubhani, M., Novikov, D., Baumgart, E., Vanhooren, J. C., Fransen, M., Goethals, M., Vandekerckhove, J., Van Veldhoven, P. P., and Mannaerts, G. P. (1996) *Eur. J. Biochem.* **240,** 660–666
31. Antonenkov, V. D., Van Veldhoven, P. P., Waelkens, E., and Mannaerts, G. P. (1997) *J. Biol. Chem.* **272,** 26023–26031
32. Katz, N., Thiele, J., and Giffhorn-Katz, S. (1989) *Eur. J. Biochem.* **180,** 185–189
33. Katz, N. R., Fischer, W., and Giffhorn, S. (1983) *Eur. J. Biochem.* **135,** 103–107
34. Twisk, J., Hoekman, M. F., Mager, W. H., Moorman, A. F., de Boer, P. A., Scheja, L., Princen, H. M., and Gebhardt, R. (1995) *J. Clin. Invest.* **95,** 1235–1243
35. Rost, B., Casadio, R., Fariselli, P., and Sander, C. (1995) *Protein Sci.* **4,** 521–533